ISSN 0280-5316
ISRN LUTFD2/TFRT--5729--SE

Friction Compensation by the use of Friction Observer

Mikael Janiec

Department of Automatic Control
Lund Institute of Technology
October 2004

Department of Automatic Control
Lund Institute of Technology
Box 118
SE-221 00 Lund Sweden

Document name
MASTER THESIS

Date of issue
October 2004

Document Number
ISRNLUTFD2/TFRT--5729--SE

Author(s)
Mikael Janiec

Supervisor
Rolf Johansson and Anders Robertsson at LTH in Lund

Sponsoring organization

Title and subtitle
Friction Compensation by the use of Friction Observer (Friktionskompensering med friktionsobserverare)

Abstract
The deteriorating effects of friction on the control of mechanical systems is a major problem in a Multitude of applications such as high-performance robotics and pointing systems. This thesis aims at improving control by using a nonlinear friction observer to detect friction in the system and use this information to modify the control input. After some initial attempts with the LuGren friction model, the observer was decided to be based on the Dahl model of friction.
Simulations and experiments were made using the unstable Furuta pendulum and the efficiency of the observer approach was compared to other standard methods for friction compensation. Although being able to serve its purpose very well in the simulated environment the observer friction compensation could not outperform the other compensation methods in the experiments, only being capable or slightly improving the control of the pendulum. The cause of this lack of success is still unclear.

Keywords

Classification system and/or index terms (if any)

Supplementary bibliographical information

ISSN and key title
0280-5316

ISBN

Language
English

Number of pages
35

Recipient's notes

Security classification

Friction Compensation by the use of a Friction Observer

Mikael Janiec

Contents

1 Introduction

1.1 Background

The deteriorating effects of friction in the control of mechanical systems is a major problem in a multitude of applications. Being able to a large extent reduce these effects is therefore of great importance. This thesis will evaluate a suggested solution to the problem consisting of the use of a friction observer based on a dynamic model of the friction. The output from the observer is then used to cancel the friction force.

1.2 Problem Formulation

The original aim of this thesis was to use the LuGre model for friction as a basis for a LuGre model observer that then later would be used to reduce the effects of friction. This first required finding an acceptable method of estimating the parameters in the model. A valiant attempt of achieving this was made, sadly without much success. The investigations of the observer approach in friction reduction instead had to be based on the not so complicated Dahl friction model. To be able to evaluate and relate the effects of the observer based friction compensation, simulations and experiments also had to be done using other methods to counter friction. As an experimental model the Furuta pendulum was chosen as the effects of friction are easy to observe and hopefully a reduced presence of the friction induced phenomena is clearly seen.

1.3 Results

When evaluated in simulations all of the investigated methods performed well. The disappointment was however great when the Dahl friction observer made an unimpressive appearance in the experiments, performing worst of all and only slightly better than with no friction compensation at all. It is also still unclear why the observer approach failed and what can be done to make the much needed improvements. After these disheartening conclusions one can only seek comfort in the consoling words of *Horátius*.

EST QUODAM PRODIRE TENUS, SI NON DATOR ULTRA

2 The Problem of Friction

For centuries friction phenomena has attracted the attention of scholars in different fields of research. In control engineering the increasing demands for controlled mechichal systems have generated a growing interest. Friction induced effects such as stick-slip motion, limit cycles and increased tracking errors severly worsen the performance thus forcing friction to be taken into accout in the control design in order to minimize the negative effects.

A couple of examples where friction limits the performace are presented below. They are borrowed from and further referenced in [5].

- Machine tooling, e.g., grinding or microdrilling with very low feed rates or oilwell drilling.
- High-performance robotics, e.g., pick-and-place machines for mounting electrical components on Printed Circuit Boards or multi-linked robots in manufacturing industry.
- Mechatronics of consumer electronic motion systems, e.g., disk drives and CD-rom players.
- Telescopes or military pointing systems.

2.1 Friction Phenomena

A lot of experimental work has been made to charachterize the different aspects of friction. The most obvious aspects of friction are described by

- Coulomb friction, a constant force independent of the velocity between the surfaces in contact acting in the opposing direction of the velocity.
- Viscous friction, a component of the friction force that increases linearly with increasing velocity.

In order to make good controller design the following qualities of a friction model in addition to the ones mentioned are however also considered to be important according to [5].

- Presliding displacement, a spring-like behaviour in the stick phase due to limited stiffness of contact aspereties.
- Static friction, independent of velocity, a function of dwell-time when sticking as well as of the rate of increase of the applied force.
- Stribeck curve, i.e., a decrease in the friction force for small velocities originating form the transition of boundary lubrication to full fluid lubrication.
- Frictional lag, a dynamic behaviour resulting in a larger friction force for increasing velocities then for decreasing becoming more apparent with large acceleration.

2.2 Static Friction Models

The classical method of modelling friction is a static map from the relative velocity of two surfaces in contact and the friction force. The map itself will consist of a combination of components modelling Coulomb, viscous and static friction as well as the Stribeck effect.[1]

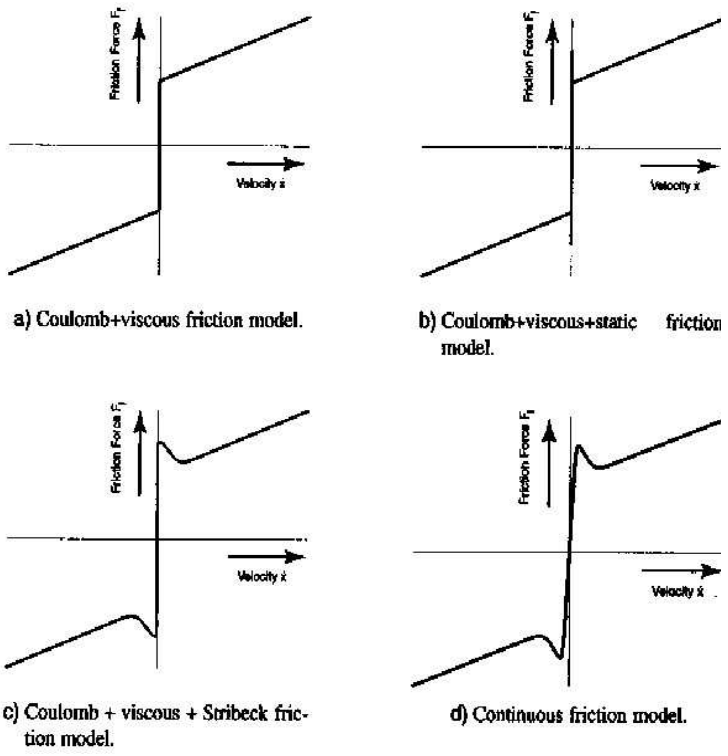

Figure 1: Various models of static friction from [5]

There are however some imperfections in the static models. The discontinuity at zero may lead to non-uniqueness of the solution to the equations of motion for the system and numerical problems when the model is used in simulation. Proposed solutions to this problem are e.g. smoothing the map by a curve with a finite slope or defining a small neighbourhood of zero velocity where the velocity is considered to be zero and the friction is a function of other forces in the system. The problem however is not completely solved by these attempts and new problems are appearing.

[1] References to original articles on these phenomena are to be found in [5]

A limitation of the classical static friction models is that they do not model presliding displacement or frictional lag, resulting in poor performance for certain regions of interest especially for low velocities and when the velocity is crossing zero. Applications where this is of importance are among others low velocity tracking and high precision positioning. An attempt to include these phenomena has been made in the *seven parameter model* but it does not seem to be appropriate for simulation purposes [5].

2.3 Dynamic Friction Models

Since the 1960's attempts have been made to capture the dynamic properties of friction by the use of dynamic models. An extra internal state that determines the level of friction in addition to the velocity is introduced. The Dahl model[2] together with its follower the LuGre friction model[1] will here be the in focus of attention and will each be alloted with a brief presentation.

2.3.1 The Dahl Model

To describe presliding displacements, Dahl exploited the differential equation to which the force-displacement curve for two objects in contact was considered to be a solution. It can in its turn be rewritten and is presented below with the addition of viscous friction.

$$\dot{z} = -\Psi(\dot{q})z + \dot{q} \tag{1}$$

$$F(z, \dot{q}) = \sigma_0 z + f_v \dot{q} \tag{2}$$

The system models the friction torque $F(z, \dot{q})$ in a joint with a relative angular velocity between the surfaces of $\dot{q}$. f_v is the viscous friction parameter, σ_0 the "stiffness" parameter and $\Psi(\dot{q}) = \frac{\sigma_0}{f_c} \mid \dot{q} \mid$, where f_c denotes the Coulomb parameter.

The Dahl model does not model the Stribeck effect or static friction and has thus limited applications, but it benefits from its relative simplicity.

2.3.2 The LuGre Model

The LuGre model has its origin in visualizing the two sliding surfaces as if they were making contact through elastic bristles deflecting like springs. If the force is sufficiently large some of the bristles will deflect so much that they will slip. The friction model is based on the average behavior of the bristles. The average bristle deflection is denoted by z and modelled by

$$\dot{z} = \dot{q} - \frac{\mid \dot{q} \mid}{g_{fr}(\dot{q})} z$$

where $\dot{q}$ is the relative velocity between the surfaces. The first term gives a deflection that is proportional to the integral of $\dot{q}$ while the second term guarantees that z approaches $z = g_{fr}(\dot{q})sign(\dot{q})$ in steady state. The function $g_{fr}(\dot{q})$

is positive and depends on material properties. $g_{fr}(\dot{q})$ will decrease monotonically from $g(0)$ when $\dot{q}$ increases and is supposed to correspond to the Stribeck effect. The friction force from the interaction of the bristles is described as

$$F(z, \dot{q}) = \sigma_0 z + \sigma_1 \dot{z} + \alpha_2 \dot{q}$$

where σ_0 is a stiffness and σ_1 is a damping coefficient and the third term is added to account for viscous friction. For $g_{fr}(\dot{q})$ the following parametrization is chosen.

$$\sigma_0 g_{fr}(\dot{q}) = f_c + (f_s - f_c)e^{-\frac{\dot{q}^2}{v_s^2}}$$

f_c and f_s is the Coulomb and stiction parameters and v_s is the Stribeck velocity. To conclude the friction model in its entirety is presented below.

$$\dot{z} = \dot{q} - \sigma_0 \frac{|\dot{q}|}{g_{fr}(\dot{q})} z \tag{3}$$

$$F(z, \dot{q}) = \sigma_0 z + \sigma_1 \dot{z} + \alpha_2 \dot{q} \tag{4}$$

$$g_{fr}(\dot{q}) = \alpha_0 + \alpha_1 e^{-\frac{\dot{q}^2}{v_0^2}} \tag{5}$$

The abillity of the LuGre model to in simulation reproduce friction phenomena such as stick-slip motion, frictional lag, presliding displacement and to cause limit cycles has been demonstrated in [1].

3 Friction Compensation

If a system has fast dynamics between the control signal and the force exerted by an actuator, the control signal is approximately proportional to the force applied. Compensation for friction can therefore be achieved by $u_{comp}(t) = u(t) + \hat{F}(t)$. $\hat{F}(t)$ is an estimate of the friction force and $u(t)$ is a control law for the system when friction is neglected.

For the static models the friction is estimated simply by using a map from the relative velocity of the surfaces in contact to the resulting friction force. The properties of the particular map of the system in question need of course first to be determined through experiments. To estimate the friction using the dynamic models an observer could be used to estimate the unknown state in the dynamic friction models. Consider the non-linear model, in our case a friction model:

$$\dot{x} = f(x, u),\ y = h(x)$$

The aim is to construct an observer such that the observer error

$$\tilde{x} = x - \hat{x}$$

converges to zero in the absence of disturbances. The simplest possible form of observer is:

$$\dot{\hat{x}} = f(\hat{x}, u) + K(y - h(\hat{x}))$$

That is the model itself with an additional correction term forcing the observer error to converge to zero even if $x(0) \neq \hat{x}(0)$.

Assuming that the structure of the model is completely known the state in the friction model observed by an observer can be utilized to determine the estimation of the friction force. The design of nonlinear observers does however not have a systematic solution and the stability of the observer error dynamics has to be investigated e.g. by Passivity or Lyapunov stability theory. An observer for the LuGre model has been proposed in [10] and the result will be presented below.

3.1 LuGre Model Friction Observer

It is first assumed that the dynamics of a system without friction is covered by the equation

$$\dot{x} = A(x) + B(x)u,\ y = C(x) \tag{6}$$

where a state vector $x \in R^n$, a control action $u \in R^1$, and A, B, C are smooth vector fields of appropriate dimensions. The feedback controller

$$u = -\phi(y) \tag{7}$$

renders the set

$$V_0 = \{x \ : \ V(x) = 0\} \tag{8}$$

of the system (6) globally asymptotically stable, provided that the function ϕ is C^1-smooth and $\phi(y)y > 0 \ \forall \ y \neq 0$; and that the system (6) is zero-state detectable.

To compensate for friction the controller (7) is now modified to

$$u = -\phi(y) + \hat{F} \tag{9}$$

where the friction estimate $\hat{F}$ is defined by the observer below.

$$\dot{\hat{z}} = \dot{q} - \sigma_0 \frac{\mid \dot{q} \mid}{g_{fr}(\dot{q})} \hat{z} + K, \ \hat{z}(0) = 0 \tag{10}$$

$$\hat{F}(\hat{z}, \dot{q}) = \sigma_0 \hat{z} + \sigma_1 \dot{\hat{z}} + \alpha_2 \dot{q} \tag{11}$$

Good choices for the variable K are given by the following statements.

THEOREM 3.1 Assume that the system (6) is passive with a proper smooth storage function V, $\min V = 0$, i.e. the time derivative of V along any solution of (6) satisfies the relation

$$\frac{d}{dt} V \leq y^T u$$

Given this system with presence of friction in the actuator of the form (3), (4) consider the controller (9) where the friction estimate $\hat{F}$ is defined by (10), (11) with

$$K = -\frac{\sigma_0}{\rho} \left[1 + \sigma_1 \frac{\mid \dot{q} \mid}{g_{fr}(\dot{q})} \right] y$$

where $\rho > 0$. Then along any solution $[x(t), z(t), \hat{z}(t)]$ of the closed loop system, the limit relation

$$\lim_{t \to \infty} V(x(t)) = 0$$

holds and $x(t)$ converges to the compact set V_0 defined in (8).

THEOREM 3.2 Assume now that the system (6) is rendered asymptotically stable with a Lyapunov function V, $\min V = 0$ where the time derivative of V along any solution of (6) satisfies the relation

$$\dot{V} \leq - \begin{bmatrix} x \\ u \end{bmatrix}^T Q(t) \begin{bmatrix} x \\ u \end{bmatrix}, \ Q = Q^T = \begin{bmatrix} Q_1 & Q_{12} \\ Q_{12}^T & Q_2 \end{bmatrix} > 0$$

Given this system with presence of friction in the actuator of the form (3), (4) consider the controller (9) where the friction estimate $\hat{F}$ is defined by (10), (11) with

$$K = -\frac{2Q_2 \left(\sigma_0 + \sigma_1 \sigma_0 \frac{|\dot{q}|}{g_{fr}(\dot{q})} \right)}{-\rho + 4Q_2 \sigma_1 \sigma_0} u$$

where $\rho > 0$. Then along any solution $[x(t), z(t), \hat{z}(t)]$ of the closed loop system, the limit relation

$$\lim_{t \to \infty} V(x(t)) = 0$$

holds and $x(t)$ converges to the compact set V_0 defined in (8).

3.2 Dahl Model Friction Observer

With the help of the observation that the LuGre model reduces to the Dahl model if $g_{fr} = f_C/\sigma_0$ and $\sigma_1 = \sigma_2 = 0$, the results from above can be made to apply for a Dahl friction observer as well. The friction estimate is now defined as

$$\dot{\hat{z}} = -\frac{\sigma_0}{f_C}(\dot{q})\hat{z} + \dot{q} + K \tag{12}$$

$$\hat{F}(\hat{z}, \dot{q}) = \sigma_0 \hat{z} + f_v \dot{q} \tag{13}$$

If the same conditions apply as in Theorem 3.1 with the exception that the friction in the actuator is on the form (1), (2) and the friction estimate is defined by (12), (13), convergence of $x(t)$ to the compact set V_0 defined in (8), is achieved with

$$K = -\frac{\sigma_0}{\rho} y.$$

With the conditions in Theorem 3.2 we instead arrive at

$$K = \frac{2Q_2\sigma_0}{\rho} u.$$

Since $Q_2 > 0$, $\sigma_0 > 0$ and the only restriction on ρ is $\rho > 0$, the coefficient in front of u can be chosen freely as long as it remains positive.

3.3 PI Controller

In mechanical systems a PI controller is often used in the control loop to compensate for disturbances on the input signal such as for example friction. The integrating part of the controller $G(s) = K + \frac{I}{s}$ will grow with time when the control signal is non-zero, acting in fact as an observer for Coulomb-type friction. The main advantages of this method of compensation is that it does not require any parameter estimation and of course is very easy to implement. This method will also later be used in simulation and experiments and its performace wil be compared to the observer approach.

4 The Furuta Pendulum

As a testing ground for our attempts of friction compensation and parameter estimation for different friction models, a process called *The Furuta Pendulum* will be used. The Furuta Pendulum is an underactuated 2 DOF system, composed of an arm rotating in the horizontal plane and to this arm a rigid pendulum is attached. They are jointed in a way that makes it possible for the pendulum to rotate in a plane perpendicular to the arm. The system is controlled by applying a torque to the arm with an electrical motor.

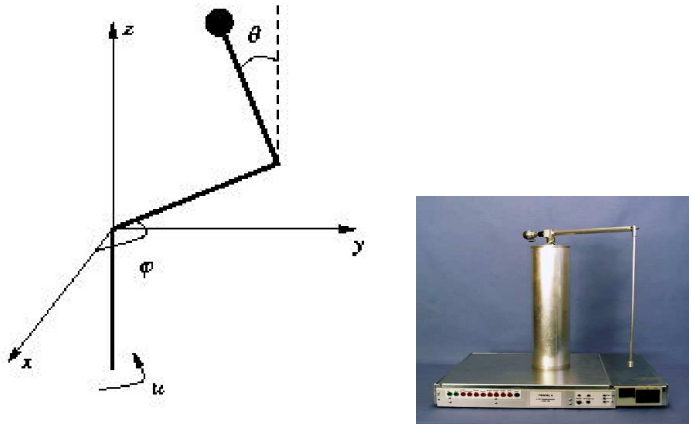

Figure 2: *(Left)* Scematic figure of the Furuta pendulum *(Right)* Photo of the Furuta pendulum

4.1 Mathematical Model

Under assumptions of point masses and no friction the equations of motion for the Furuta pendulum are

$$M(q)\ddot{q} + C(q,\dot{q})\dot{q} + G(q) = \tau$$

where $q = [\theta, \phi]^T \in S^1 \times S^1$, ϕ is the angle of the arm moving in the horizontal plane and θ is the angle of the pendulum measured from its upright position. Further more

$$M(q) = \begin{bmatrix} m_2 l_2^2 & m_2 l_1 l_2 \cos\theta \\ m_2 l_1 l_2 \cos\theta & m_1 l_1^2 + m_2(l_1^2 + l_2^2)\sin^2\theta \end{bmatrix},$$

$$C(q,\dot{q}) = m_2 \begin{bmatrix} 0 & l_2^2\dot{\phi}\cos\theta\sin\theta \\ (l_2^2\dot{\phi}\cos\theta - l_1 l_2)\sin\theta & l_2^2\dot{\theta}\cos\theta\sin\theta \end{bmatrix},$$

$$G(q) = \begin{bmatrix} -g m_2 l_2 \sin\theta \\ 0 \end{bmatrix}$$

and finally

$$\tau = \begin{bmatrix} 0 \\ u \end{bmatrix}.$$

m_1 and m_2 are the masses of the arm and pendulum respectivly, l_1 and l_2 are the distances from the center of mass of the arm and pendulum to their suspension points and u is the control input.

4.2 Control of the Pendulum

Before the methods of friction parameter estimation are investigated an appropriate controller that has to be chosen. Not only does it have to be suitable for friction compensation experiments, but to be able to exploit the observers from the previous section to compensate for friction, the method of control has to meet the requirements stated in Theorem 3.1 or 3.2. A controller that stabilizes the pendulum in its upright position for a desired position or angular velocity of the rotating arm seems to be suitable to evaluate the friction compensation. Under these conditions the principal dynamics of the pendulum are assumed to be captured by its linearized form. First the design of a controller stabilizing both arm and pendulum is considered. Introducing a state vector $(\ \theta \quad \dot{\theta} \quad \phi - \phi_0 \quad \dot{\phi} \ )^T$ the system (4.1) is linearized around the operating point $(\ 0 \quad 0 \quad 0 \quad \dot{\phi}_0 \ )^T$, where $\dot{\phi}_0$ in this case is being zero. The result is presented below.

$$\begin{bmatrix} \dot{\theta} \\ \ddot{\theta} \\ \dot{\phi} \\ \ddot{\phi} \end{bmatrix} = \begin{bmatrix} 0 & 1 & 0 & 0 \\ \frac{ab\dot{\phi}^2+bd}{ab-c^2} & 0 & 0 & 0 \\ 0 & 0 & 0 & 1 \\ \frac{-ac\dot{\phi}^2-cd}{ab-c^2} & 0 & 0 & 0 \end{bmatrix} + \begin{bmatrix} 0 \\ \frac{-c}{ab-c^2} \\ 0 \\ \frac{a}{ab-c^2} \end{bmatrix}$$

where $a = m_2 l_2$, $b = m_1 l_1^2 + m_2 l_1^2$, $c = m_2 l_1 l_2$ and $d = g m_2 l_2$.

The control law can be written as

$$u = -\begin{bmatrix} \ l_1 & l_2 & l_3 & l_4 \ \end{bmatrix} \begin{bmatrix} \theta \\ \dot{\theta} \\ \phi - \phi_0 \\ \dot{\phi} \end{bmatrix}$$

The state feedback parameters are calculated by the use of LQ design. The weighting matrices are chosen as below.

$$Q = \begin{bmatrix} 100 & 0 & 0 & 0 \\ 0 & 1 & 0 & 0 \\ 0 & 0 & 5 & 0 \\ 0 & 0 & 0 & 0.1 \end{bmatrix}$$

$$R = 70$$

For the velocity tracking controller the state ϕ is irrelevant. The state space vector $(\ \theta \quad \dot{\theta} \quad \dot{\phi} - \dot{\phi}_0 \ )^T$ is introduced and the linearized system rewritten as

$$\begin{bmatrix} \dot{\theta} \\ \ddot{\theta} \\ \ddot{\phi} \end{bmatrix} = \begin{bmatrix} 0 & 1 & 0 \\ \frac{ab\dot{\phi}^2+bd}{ab-c^2} & 0 & 0 \\ \frac{-ac\dot{\phi}^2-cd}{ab-c^2} & 0 & 0 \end{bmatrix} + \begin{bmatrix} 0 \\ \frac{-c}{ab-c^2} \\ 0 \\ \frac{a}{ab-c^2} \end{bmatrix}$$

The new control law is

$$u = -\begin{bmatrix} l_1 & l_2 & l_3 \end{bmatrix} \begin{bmatrix} \theta \\ \dot{\theta} \\ \dot{\phi} - \dot{\phi}_0 \end{bmatrix}$$

Again the parameters are calculated with LQ design, with the choice of weighting matrices presented below.

$$Q = \begin{bmatrix} 100 & 0 & 0 \\ 0 & 1 & 0 \\ 0 & 0 & 10 \end{bmatrix}$$

$$R = 60$$

As can be seen from the equations the linearization and thereby the controller parameters are highly sensitive to changes in the desired angular velocity, $\dot{\phi}_0$. Therefore the state feedback parameters constantly have to be recalculated with changing reference signal. A switch also has to be made between velocity and position tracking when the reference signal is set to zero.

4.3 Stability of the Observer in the Closed-Loop System

Consider a linear system system $\dot{x} = Ax + Bu$, $y = Cx$, controlled with state feedback, $u = -Lx$, where if the states are available $L = R^{-1}B^TS$, where S satisfies the the equation $A^TS + SA - SBR^{-1}B^TS + Q = 0$, $Q \geq 0$ and $R > 0$. It is then known from LQ theory that $V(x) = x^TSx$ is a Lyapunov function fulfilling the conditions for Lyapunov stability. In the case of the position control of Furuta pendulum the Lyapunov function is:

$$V(x) = x^T \begin{bmatrix} 40.5946 & 6.4988 & 8.3659 & 4.0333 \\ 6.4988 & 1.4414 & 1.7638 & 0.9111 \\ 8.3659 & 1.7638 & 3.4648 & 1.1505 \\ 4.0333 & 0.9111 & 1.1505 & 0.5883 \end{bmatrix} x$$

So if the pendulum were a linear system the conditions in Theorem 3.2 would be met. Since the controller in the case of the Furuta pendulum is based on the linearized model neither the stability of the system with nor without a friction observer is certain. One may however argue that the pendulum probably can be put in an almost linear form (See [3]), thereby granting stability, at least in a small region.

5 Identification of Friction Model Parameters

5.1 Friction Force Estimation

An obvious problem when dealing with the characterization of friction in a system is that the generated friction force is not directly measurable. In order to solve this problem the simplest possible method will be used. The dynamics between the control signal and the exerted force in the Furuta Pendulum are fast and therefore the following relation between the friction force, $F(t)$ and the control signal, $u(t)$ holds: $u_{real}(t) = u(t) - F(t)$. Together with the system equations for the pendulum (4.1) it is now possible to calculate the friction force if only $\ddot{\theta}$ or $\ddot{\phi}$ are known. This of course requires numerical differentiation of an observable state, thus running the risk of calculating numerical derivatives. Both simulations and experiments show however that the performance of the estimator is acceptable when using the differentiated $\dot{\theta}$ in the calculations.

5.2 Identification of the Parameters in a Static Friction Model

A simple static friction model, only dealing with Coulomb and viscous friction, will be considered and later used in simulations and experiments.

$$F = f_c sign(\dot{\phi}) + f_v \dot{\phi}$$

F is the friction force, f_c and f_v are the parameters for Coulomb and viscous friction respectively. The friction force according to this model at each point in time is thereby given by

$$F_t = \begin{bmatrix} f_c & f_v \end{bmatrix} \begin{bmatrix} sign(\dot{\phi}_t) \\ \dot{\phi}_t \end{bmatrix}$$

Seen in this form the equation can be used in a recursive least-squares algorithm to estimate the parameters in the model, exploiting measurements of the observed variable F_t and the regressor vector $\begin{pmatrix} sign(\dot{\phi}_t) & \dot{\phi}_t \end{pmatrix}^T$.

There is no guarantee that the friction parameters are the same in both directions, it may be wise to separate the estimation for positive and negative velocities.

It is also probably best not to use measurements in the vicinity of $\dot{\phi} = 0$. Both the measured angular velocity and the estimated friction are probably very uncertain in this region and it is better to exclude the data altogether from the calculations.

5.3 Identification of the Parameters in the Dahl Model

To be able to estimate the parameters in the Dahl model the equations (1) and (2) have to be written in discrete form. This is made using the backward Euler method, replacing $\frac{d}{dt}$ with $\frac{q-1}{hq}$, arriving at the equations below.

$$z_t = \left(1 - \frac{\sigma_0}{f_c} \mid \dot{\phi}_{t-1} \mid h\right) z_{t-1} + h\dot{\phi}_{t-1} = \Phi z_{t-1} + \Gamma \dot{\phi}_{t-1}$$

$$F = \sigma_0 z_t + f_v \dot{\phi}_t = C z_t + D \dot{\phi}_t$$

The pulse-transfer operator, $H(q)$, for the state space model above is given by the relation

$$H(q) = C\left(qI - \Phi\right)^{-1}\Gamma + D$$

The input-output relationship between angular velocity $\dot{\phi}$ and friction force F can thus be written as

$$F_t - F_{t-1} = -\frac{\sigma_0}{f_c} h \mid \dot{\phi}_{t-1} \mid F_{t-1} + f_v \dot{\phi}_t + \left(\sigma_0 h - f_v\right)\dot{\phi}_{t-1} + f_v \frac{\sigma_0}{f_c} h \mid \dot{\phi}_{t-1} \mid \dot{\phi}_{t-1}$$

Introducing new names for the parameters

$$F_t - F_{t-1} = \alpha \mid \dot{\phi}_{t-1} \mid F_{t-1} + \beta \dot{\phi}_t + \gamma \dot{\phi}_{t-1} + \delta \mid \dot{\phi}_{t-1} \mid \dot{\phi}_{t-1} \tag{14}$$

This can be rewritten on a form which directly can be used in a recursive least-squares algorithm, with an observed variable $F_t - F_{t-1}$, parameter vector $\begin{pmatrix} \alpha & \beta & \gamma & \delta \end{pmatrix}$ and regressor vector $\begin{pmatrix} \mid \dot{\phi}_{t-1} \mid F_{t-1} & \dot{\phi}_t & \dot{\phi}_{t-1} & \mid \dot{\phi}_{t-1} \mid \dot{\phi}_{t-1} \end{pmatrix}^T$.

$$F_t - F_{t-1} = \begin{bmatrix} \alpha & \beta & \gamma & \delta \end{bmatrix} \begin{bmatrix} \mid \dot{\phi}_{t-1} \mid F_{t-1} \\ \dot{\phi}_t \\ \dot{\phi}_{t-1} \\ \mid \dot{\phi}_{t-1} \mid \dot{\phi}_{t-1} \end{bmatrix}$$

The estimated parameters in the friction model are given by the relations $f_c = \frac{\delta+\beta}{\alpha}$, $f_v = -\frac{\gamma}{\alpha}$ and $\sigma_0 = \frac{\delta+\beta}{h}$.

Again there may be a point in separating the estimation for movements in the positive and negative direction.

A problem with the use of LS to identify parameters in a dynamic model is that the estimate not always will be consistent, that is converging to its true value with an increasing amount of data. This is the case when the noise in the measurements is coloured. As this is something that can not be ruled out the estimates provided by the method above must be considered uncertain. They are however the best at hand.

5.4 Identification of Parameters in the LuGre Model

A method of identifying the parameters of the LuGre model in a series of experiments has ben outlined by Canudas de Wit. There were however no easy recursive methods described to estimate the LuGre model parameters at the beginning of this masters thesis and sadly there are, after an substantial amount of effort, still none. This limits the usefullness of the LuGre model in making friction compensation without the need of first making a set of specialized experiments. This model will therefore not be investigated further.

6 Simulation

Simulations of the Furuta pendulum were made in the MATLAB Simulink environment using an existing model for the pendulum together with the controller, a friction model, a friction observer and a friction parameter estimator, all given an introduction in the previous sections.

6.1 Furuta Pendulum without Friction

The Furuta pendulum controlled with the earlier mentioned LQ derived state feedback controller is simulated with a initial value of the pendulum position of 0.1 rad. The realization for both position and velocity tracking modes is presented in Figure 3.

In a position tracking situation the dotted line will henceforward represent the deviation of the pendulum from its upright position in radians and the solid line the deviation of the arm from its starting position. When performing velocity tracking the solid line is the measured angular velocity and the dotted line is the desired angular velocity. The function $sin(-\frac{\pi}{10}t)$ is used in all of the simulations and later also the experiments as the desired angular velocity. This choise is made because of the clearly deteriorating effect that the friction has when using it as the reference signal, making the compensation easy to evaluate.

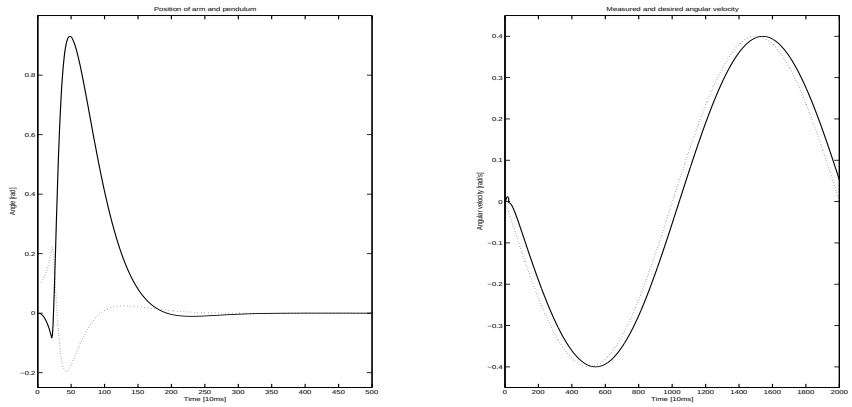

Figure 3: *(Left)* Simulation of the Furuta pendulum, $\dot{\phi}_{ref} = 0$. The solid line represents the position of the arm and the dotted line the position of the pendulum. *(Right)* Simulation of the Furuta, $\dot{\phi}_{ref} = \sin(-\frac{\pi}{10}t)$. The solid line represents the angular velocity of the arm and the dotted line the reference signal.

6.2 Furuta Pendulum with Coulomb and Viscous Friction

Friction simulated from a static friction model with $f_c = 0.1$ and $f_v = 0.04$ is added to the control signal in the system. To get a smooth zero velocity transition the friction signal is fed through a low pass filter $G(s) = \frac{1}{0.01s+1}$. As one can expect the non-linearity of the friction model induces a limit cycle when attempting to hold the pendulum upright. An offset appears between the desired and measured angular velocity when simulating velocity tracking. This is shown in Figure 4. The friction force during the limit cycles is shown in Figure 5.

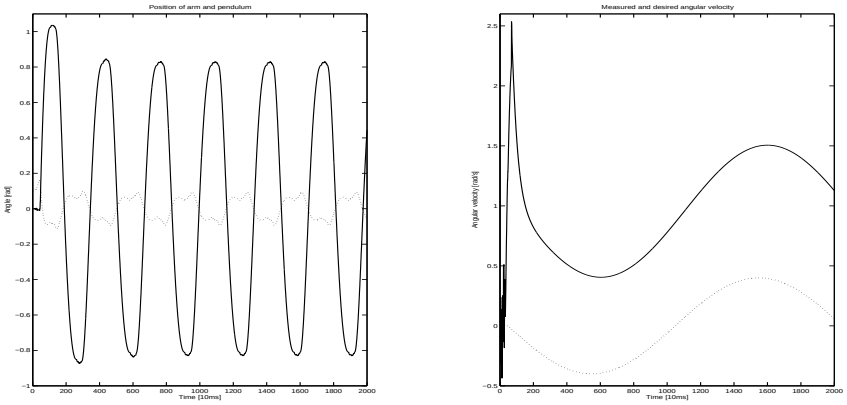

Figure 4: *(Left)* Simulation of the Furuta pendulum with static friction, $\dot{\phi}_{ref} = 0$. *(Right)* Simulation of the Furuta pendulum with static friction, $\dot{\phi}_{ref} = \sin(-\frac{\pi}{10}t)$.

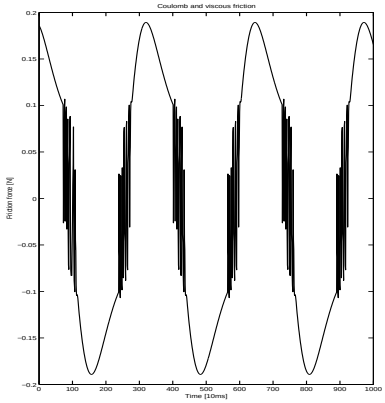

Figure 5: Static friction

Now, compensation for the friction is added. This is achieved by using the same map as the simulated friction but with an additional dead zone for $\dot{\phi} <|$ 0.01 | to avoid some of the erratic behaviour in the zero crossings. First the parameter estimated and the estimates are given some time to converge before the estimation is switched off to avoid problems with closed loop identification. The compensation is then activated. The result for the position and velocity tracking is seen in Figure 6.

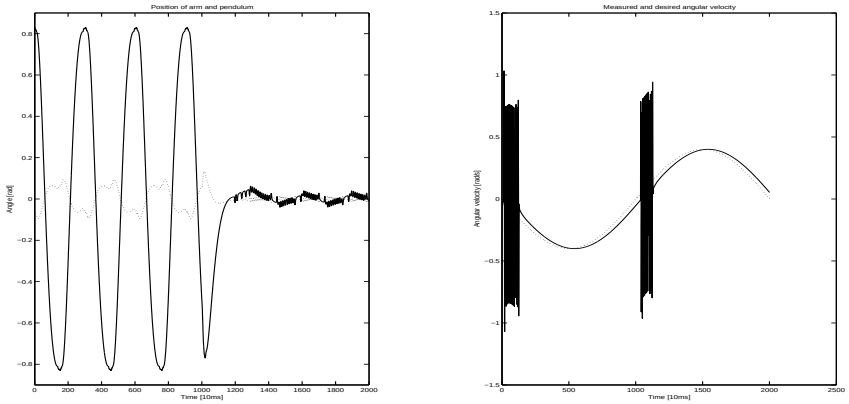

Figure 6: *(Left)* Simulation of the Furuta pendulum with compensated static friction, $\dot{\phi}_{ref} = 0$. *(Right)* Simulation of the Furuta pendulum with compensated static friction, $\dot{\phi}_{ref} = \sin(-\frac{\pi}{10}t)$.

6.3 Furuta Pendulum with Dahl Friction

The simulated friction in the system is coming from the Dahl model with $f_c = 0.1$, $f_v = 0.04$ and $\sigma_0 = 2$. Again a limit cycle or an offset between desired and measured angular velocity appears in the simulations as demonstrated in Figure 7. The friction force during the limit cycles is shown in Figure 8.

6.3.1 Compensation using the Friction Observer

The Dahl friction observer is applied to counter the effects of friction. The correction term in the observer is chosen as $K = 1.5 \cdot 10^4 u$. An overview of the Simulink block diagram is given in Figure 9.

The estimated parameters are as earlier allowed to converge to their true values before compensation from the friction observer is switched on again to avoid possible problems with closed-loop estimation. The total success of the compensation for both methods of control is proudly presented in Figure 10.

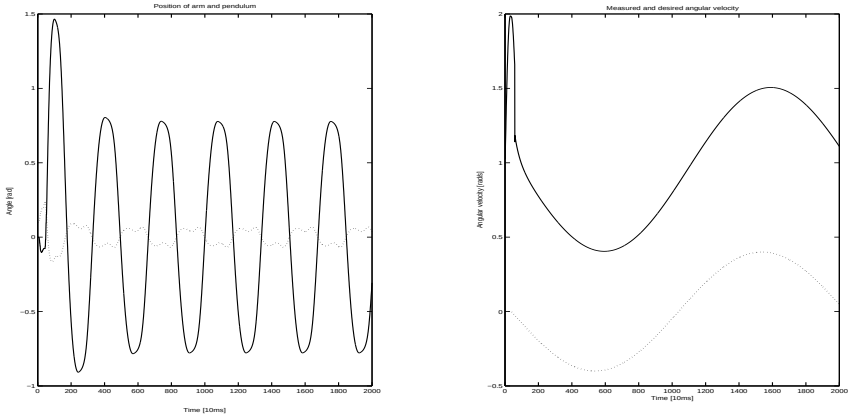

Figure 7: *(Left)* Simulation of the Furuta pendulum with Dahl friction, $\dot{\phi}_{ref} = 0$. *(Right)* Simulation of the Furuta pendulum with Dahl friction, $\dot{\phi}_{ref} = \sin(-\frac{\pi}{10}t)$.

6.3.2 Compensation using a PI Controller

The control signal from the state-feedback controller is now fed through a PI contoller with $G(s) = 1 + \frac{30}{s}$, before it is allowed to act on the process. Once again as seen in Figure 11 an efficient method of dealing with the friction in the system has been found.

6.3.3 Compensation using the Estimated Friction

One may wonder why one should bother with the estimation of the parameters of a friction model and then use an observer when the friction itself has to be estimated, as described in section 5.1, in order to estimate the parameters. If the signal from the estimator used directly as compensation the simulation is unstable. When filtering the signal from the friction estimator through a saturation followed by a low pass filter $G(s) = \frac{1}{0.01s+1}$, before applying it the result is stable and indeed almost identical to the one seen with previous methods. This is shown in Figure 12.

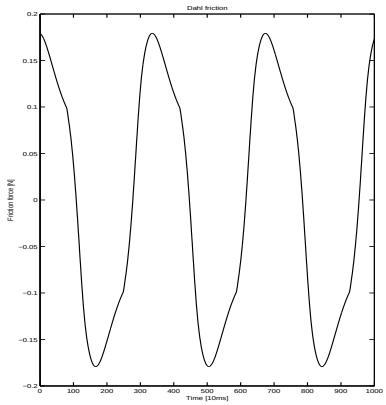

Figure 8: Dahl friction

7 Experiments

The very promising results from the simulations now have to be confirmed in the real world. Experimental evaluation was made on the Furuta pendulum at the Robot lab of the control department. MATLAB Simulink programming was again utilized for implementation. A detailed presentation of the hardware and its Simulink interface is given in [12].

In an attepmt to objectively measure the performance of the different friction compensation methods the cost function from the LQ controller calculations will be used as a penalty function. That is,

$$J = \frac{1}{T} \int_0^T x^T Q x + uRu \, dt$$

with the same Q and R as was used earlier. The integration will be made over a time period of 20 seconds.

The sampling period will be 10 ms for all of the experiments. The linearized system equations for the pendulum are with the help of MATLAB discretized for this sample time before the state-feedback parameters are determined. Due to reasons not fully understood the control signal from the state-feedback has to be scaled with a gain of 2 to be able to keep the pendulum upright.

7.1 No Friction Compensation

The movement of the state feedback controlled pendulum is presented in Figure 13, with the solid and dotted line representing the position of arm and pendulum as earlier. The same type of limit cycles that are recognized from the simulations appear, together with an offset between the desired an measured angular velocity

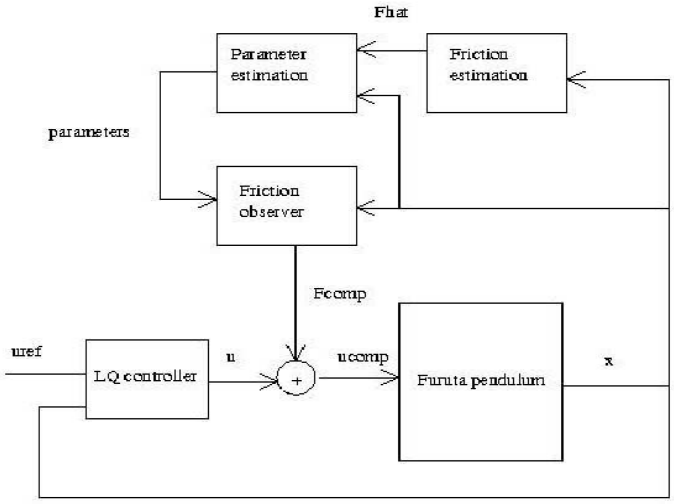

Figure 9: Simulink block diagram.

in a velocity tracking experiments. The estimated friction during the limit cyles is shown in Figure 7.1. Here too the form of the curve resembles the simulation results.

The amplitude of the arm oscillations is smaller than in the simulations as an effect of the up-scaled control signal. One obvious difference is also that there is no symmetry in the limit-cycles around $\phi = 0$. This is probably due to the fact that the pendulum is slightly bent and the same phenomenon will appear everywhere and haunt all of the experiments. The value of the penalty function is $J = 1.255$ and will be remembered as a reference.

7.2 Compensation Using Static Friction Model

An attempt to compensate for the friction force is made using the same static friction model as before, this time a total of four parameters, two for each direction of the velocity is estimated and used in the model. The parameter estimation is switched off when the parameter estimates have settled and compensation is then activated, thus avoiding problems with closed-loop estimation. The change in the behaviour of the pendulum can be seen in Figure 15. Again the lack of symmetry in the limit-cyles is obvious and probably deteriorates the result. The somewhat improved performance is however confirmed by the fact that $J = 0.934$. The result is not as good as in the simulation something that is not at all surprising due to the use of a very crude friction model that is far from the real friction.

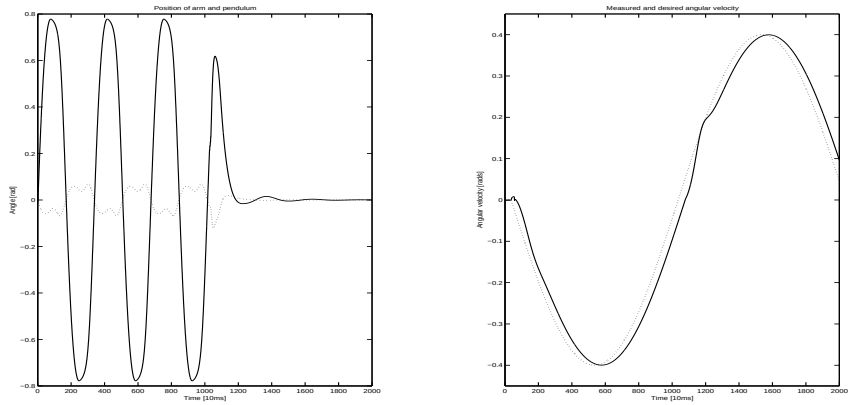

Figure 10: *(Left)* Simulation of the Furuta pendulum with Dahl friction and observer compensation, $\dot{\phi}_{ref} = 0$. *(Right)* Simulation of the Furuta pendulum with Dahl friction and observer compensation, $\dot{\phi}_{ref} = \sin(-\frac{\pi}{10}t)$.

7.3 Compensation using a PI Controller

In the same manner as in the simulation the control signal from the state-feedback controller is subjected to PI control. This time the parameters are $G(s) = 1 + \frac{60}{s}$. To avoid instabillity the integration part is slowly ramped up to the final value. The behaviour of the pendulum with this controller can be seen in Figure 16. The penalty function is now $J = 0.697$ and the method consequently proves itself on the lab process as well. This may already seem to be good but due to the flaw in the lab equipment that forces the arm to constantly have an offset from its zero value the result is actually even better.

7.4 Compensation using Friction Feedback

Again as in the simulation the output from the friction estimator from 5.1 is fed through a saturation and the low pass filter $G(s) = \frac{1}{0.05s+1}$ and added to the control signal. The success of the metod in the simulations is repeated as seen in Figure 17. The penalty function takes the value of $J = 0.512$. It is possible to improve the results even more by chosing another filter. Typically the limit cycles tend to have smaller amplitude when a filter with a higher cut-off frequency is used. The opposite applies to the velocity tracking situation where a lower breaking point is preferred.

7.5 Compensation Using Dahl Friction Observer

So far there have been some excellent results which increases the expectations for the observer method. One would expect that the most complicated metod

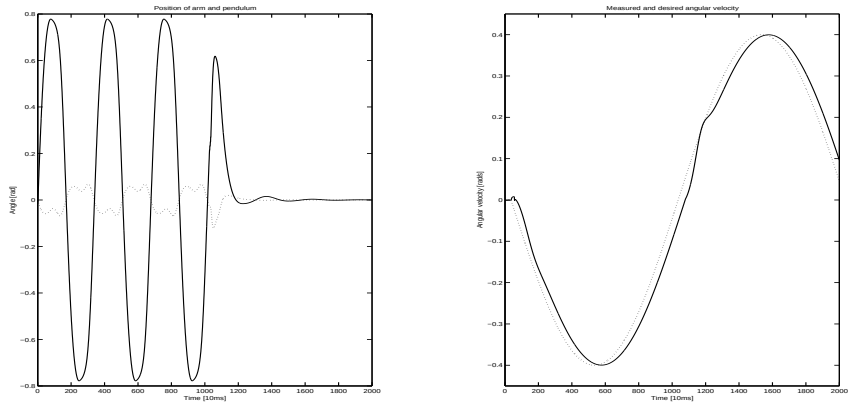

Figure 11: *(Left)* Simulation of the Furuta pendulum with Dahl friction and PI compensation, $\dot{\phi}_{ref} = 0$. *(Right)* Simulation of the Furuta pendulum with Dahl friction and PI compensation,$\dot{\phi}_{ref} = \sin(-\frac{\pi}{10}t)$.

of friction compensation would also have best performace. Sadly this is however not the case. The effect that the observer compensation has on the process is presented in Figure 18. The parameter estimates are first allowed to settle before the estimation is switched off and compensation activated, as mentioned before to avoid problems with closed loop estimation. The optimal correction term in the observer is seen to be $K = 0.2u$. Our objective method chosen to measure success, the penalty function, says that we would almost be better of without compensation as $J = 1.055$, reducing the value with a mere 15 percent. The output from the observer is shown as a solid line in Figure 19 together with te estimated friction as a dotted line.

The congruence is not very good neither when compensation is active nor when it is not. While inactivated the observer tends to drift away from the estimated friction and does not seem to be able to model the friction. When active it appears as if the observer is not fast enough to keep up with the more rapid changes in the friction although the observer curve now resembles the one of the estimated friction.

So, where could the method have gone wrong? Some of the probable weak spots of the Dahl observer approach and possible causes to the lack of good performance are presented below.

- The frist that comes to mind is that the friction model may be to far from reality to be utilized in an observer. The discrepancy in the model can be observed by comparing the behaviour of the friction force in simulations and in experiments seen in Figure 8 and Figure 7.1.
- As already pointed out the parameter estimates were suspected to be uncertain something that is confirmed in experiments where the parameter estimates does not converge to the same values for every experiment.

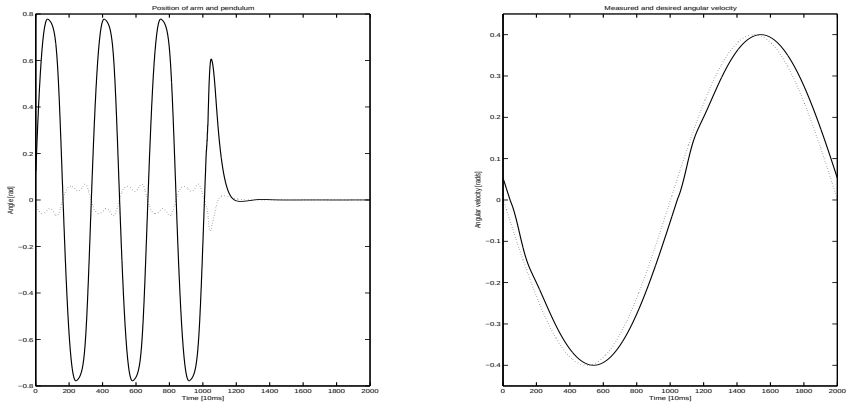

Figure 12: *(Left)* Simulation of the Furuta pendulum with state feedback controller, $\dot{\phi}_{ref} = 0$. *(Right)* Simulation of the Furuta pendulum with state feedback controller, $\dot{\phi}_{ref} = \sin(-\frac{\pi}{10}t)$.

- The friction model may be accurate but the observer structure itself not adequate. As seen in Figure 19 the observer is clearly not fast enough to counter a rapidly changing friction force.
- Finally imperfections in the lab equiment such as measurment noise, limitations in sampling rate or model error in the pendulum itself may have a halting effect on the observer.

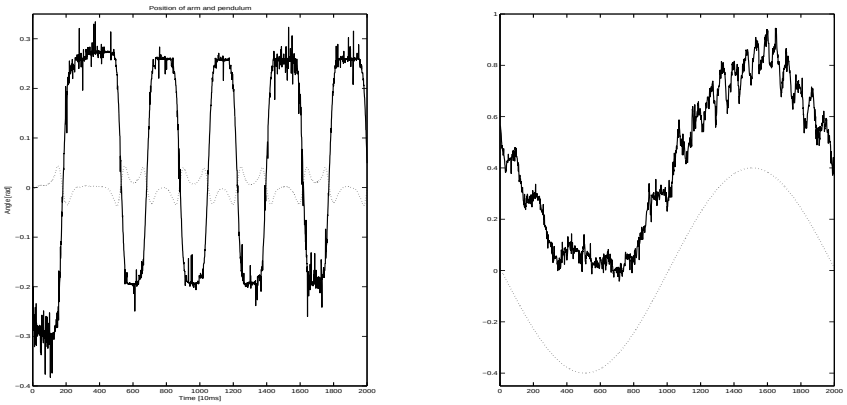

Figure 13: *(Left)* The real Furuta pendulum without friction compensation, $\dot{\phi}_{ref} = 0$. *(Right)* The real Furuta pendulum without friction compensation, $\dot{\phi}_{ref} = \sin(-\frac{\pi}{10}t)$.

8 Conclusions

One has to conclude that the methods of friction compensation for the Furuta pendulum based on a friction model, static or dynamic, could not match the success of the easy implementable PI controller and the friction estimator. Although all of the evaluated methods worked well in simulation the experiments on the real process clearly demonstrated the inferior performance of the friction observer compensation. The reasons for this remain unclear. It is possible that the relative long sample time of 10 ms that was used is too slow for the fast dynamics of the friction. This could not be tested due to the limitations in the computer hardware. Measurement noise is also a factor that could have had a negative influence on especially the parameter estimation and it would therfore be a good idea to try to reduce the different sources of disturbances. However it is far from obvoius that these actions would dramatically improve the performance of the observer. The method of using the estimated friction for compensation was a success in spite of using the same relatively long sample time and having to differentiate a noisy signal.

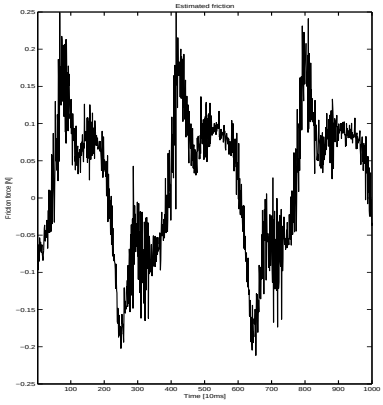

Figure 14: Estimated friction in the real Furuta pendulum.

References

[1] Canudas de Wit C., Olsson H., Åström K. J. and Lischinsky P. *A New Model for Control Systems with Friction* IEEE Trans. on Automatic Control, 40(3), 419-425, 1995

[2] Dahl P. *A Solid friction model* Aerospace Corp., El Segundo, CA, Tech. Rep. TOR-0158(3107-18)-1, 1968

[3] Glad T., Ljung L. *Reglerteori* Studentlitteratur, 2003

[4] Gäfvert M. *Comparison of two Friction Models* MSc thesis, Department of Automatic Control, Lund Institute of Technology, 1996

[5] Hensen Ronnie H.A. *Controlled Mechanical Systems with Friction* PhD thesis, Technische Universiteit Eindhoven, 2002

[6] Johansson R. *System Modeling and Identification* Prentice Hall, 1993

[7] Objer L., Holst U., Holst J. *Tidsserieanalys* LTH, 2002

[8] Olsson H. *Control Systems with Friction* PhD thesis, Department of Automatic Control, Lund Institute of Technology, 1996

[9] Olsson H., Åström K. J. *Observerer-Based Friction Compensation* Proceedings of the 35th Conference on Decision and Control, Kobe, Japan, 1996

[10] Shiriaev A.S., A. Robertsson and R. Johansson. *Friction Compensation for Passive Systems Based on the LuGre Model* 2nd IFAC Workshop on Lagrangian and Hamiltonian Methods for Nonlinear Control, Seville 2003

[11] Shiriaev A.S., L. Paramonov, A. Sørensen and A. Robertsson. *Stabilization of Rotational Modes for the Furuta Pendulum*

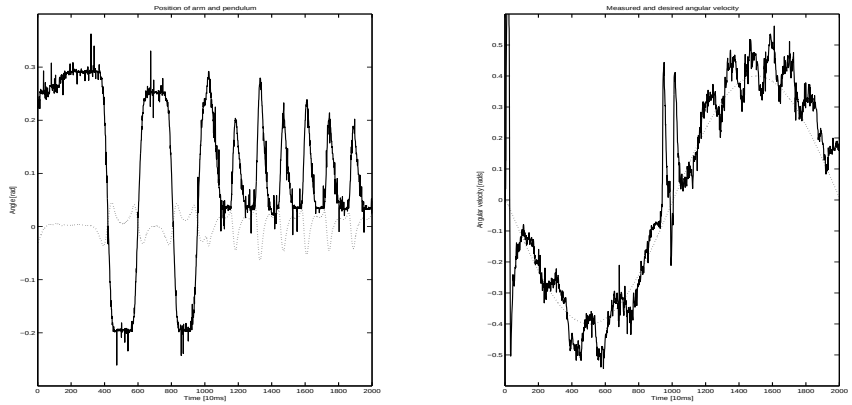

Figure 15: *(Left)* The real Furuta pendulum with static friction compensation, $\dot{\phi}_{ref} = 0$. *(Right)* The real Furuta pendulum with static friction compensation, $\dot{\phi}_{ref} = \sin(-\frac{\pi}{10}t)$.

[12] Åkesson J. *Safe Manual Control of Unstable Systems* MSc thesis, Department of Automatic Control, Lund Institute of Technology, 2000

[13] Åström K. J., Wittenmark B. *Adaptive Control* Addison-Wesley, 1995

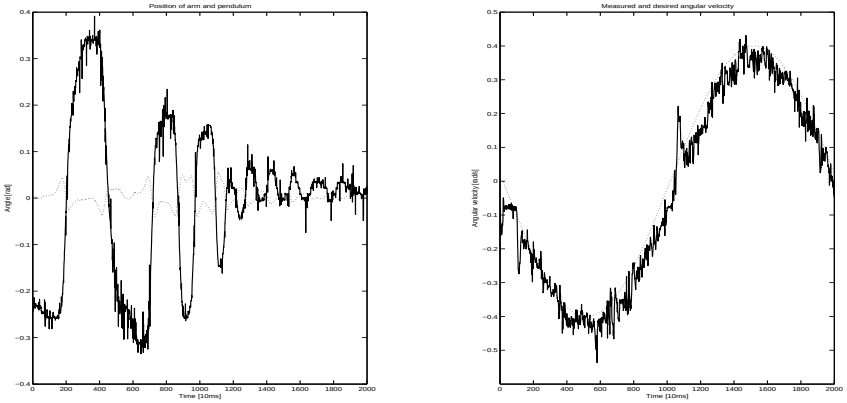

Figure 16: *(Left)* The real Furuta pendulum with PI control, $\dot{\phi}_{ref} = 0$. *(Right)* The real Furuta pendulum with PI contol, $\dot{\phi}_{ref} = \sin(-\frac{\pi}{10}t)$.

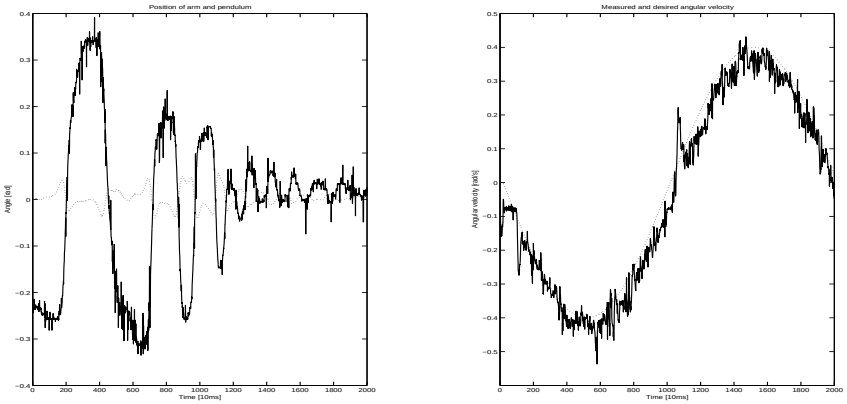

Figure 17: *(Left)* The real Furuta pendulum using estimated friction as compensation, $\dot{\phi}_{ref} = 0$. *(Right)* The real Furuta pendulum using estimated friction as compensation, $\dot{\phi}_{ref} = \sin(-\frac{\pi}{10}t)$.

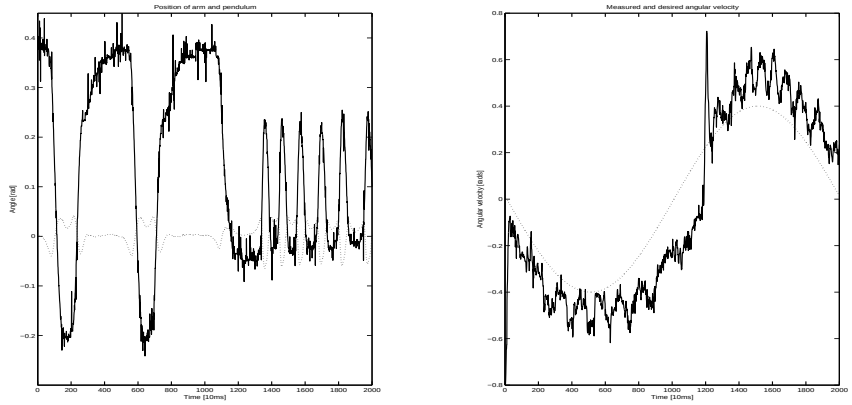

Figure 18: *(Left)* The real Furuta pendulum using Dahl friction observer for compensation, $\dot{\phi}_{ref} = 0$. *(Right)* The real Furuta pendulum using Dahl friction observer for compensation, $\dot{\phi}_{ref} = \sin(-\frac{\pi}{10}t)$.

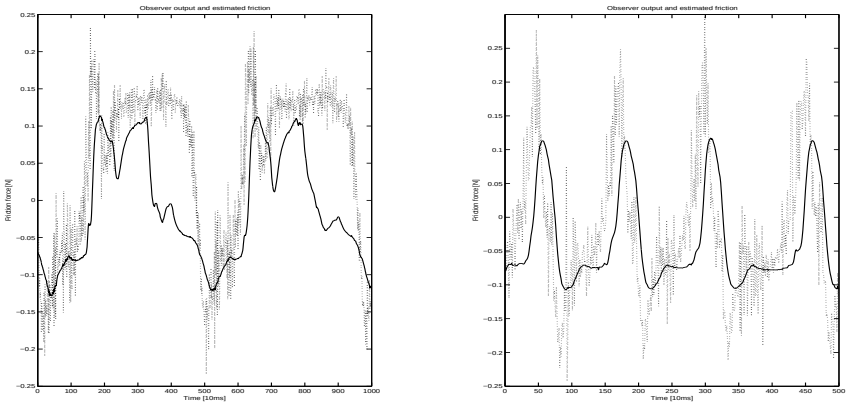

Figure 19: *(Left)* Dahl friction observer and estimated friction when compensation is inactivated, $\dot{\phi}_{ref} = 0$. *(Right)* Dahl friction observer and estimated friction when compensation is activated, $\dot{\phi}_{ref} = 0$.